Journal of the Physical Society of Japan
Vol. 66, No. 4, April, 1997, pp. 957-960

Interplay of Spin and Orbital Orderings in Perovskite Manganites

Wataru KOSHIBAE, Yuhki KAWAMURA[1], Sumio ISHIHARA[2], Satoshi OKAMOTO[1], Jun-ichiro INOUE[1] and Sadamichi MAEKAWA[1,3]

Center for Integrated Research in Science and Engineering, Nagoya University, Nagoya 464-01
[1]*Department of Applied Physics, Nagoya University, Nagoya 464-01*
[2]*Department of Applied Physics, University of Tokyo, Tokyo 113*
[3]*Institute for Materials Research, Tohoku University, Sendai 980-77*

(Received December 18, 1996)

We present an exact diagonalization study for perovskite manganites using an effective Hamiltonian which includes a coupling between the spin and orbital degrees of freedom derived from a strong on-site Coulomb interaction and orbital degeneracy of Mn ions. We investigate spin and orbital orderings as well as their excitations for the undoped insulating and the doped charge-ordered phases using three-dimensional $2 \times 2 \times 2$ clusters to maintain proper symmetry of the systems. It is shown that the anisotropic magnetic structures, such as A-type antiferromagnetic ordering, are realized by self-adjustment of the orbital ordering where the orbital degeneracy is lifted by spins, indicating a strong interplay of spins and orbitals.

KEYWORDS: Mn oxides, orbital ordering, exact diagonalization, strongly correlated electron systems

Doped perovskite manganites have recently become the focus of renewed interest because of the colossal magnetoresistance (CMR) observed in the ferromagnetic (F) metal phase[1-3] and in the 50%-doped charge-ordered phases of, for example, $La_{0.5}Ca_{0.5}MnO_3$ and $Pr_{0.5}Sr_{0.5}MnO_3$.[4,5] The CMR effect is more dramatic in the latter case than in the former. This is nothing but an insulator-metal transition by magnetic fields. The phase diagrams of the manganites $(R_{1-x}A_x)MnO_3$, where R is, for example, Pr or La, and A is Ba, Ca or Sr, show a rich variety of magnetic properties.[5-9] Undoped manganites, *e.g.*, $LaMnO_3$, are antiferromagnetic (AF) insulators with a layered spin structure, A-type AF. The metallic F phase appears in the region of $0.1 < x \lesssim 0.5$, while the region shrinks for smaller average ionic radii $\langle r \rangle$ of R and A ions. In the region of $0.5 \lesssim x \leq 1.0$, various types of AF ordering, such as the stripe-type AF (C-type AF), usual alternate-type AF (G-type AF) and a complex spin and charge-ordered phase AF (CE-type AF), appear.

A recent survey of materials to elucidate the mechanism of the CMR effect suggests that the CE-type AF appears in a rather narrow range of $x \sim 0.5$, and that even the A-type AF ordering exists near the metallic F phase in the region of $x \sim 0.5$ when the average ionic radius is large.[4,10-12] Because the CMR effect is closely related to the magnetic state, and the insulator-metal transition driven by relatively weak magnetic fields suggests that magnetically ordered phases are nearly degenerate, it may be crucial to clarify the origin of the appearance of these various magnetic states to understand the CMR effect. In this paper, using the exact diagonalization (ED) method developed recently for understanding high-temperature superconductivity, we will show that an interplay of spins and orbitals, originating from the orbital degeneracy of Mn ions and the strong on-site Coulomb interaction, is decisive for the magnetic orderings.

We start with the ionic model of Mn ions to describe the electronic states of manganites with emphasis on the role of the on-site Coulomb interaction. The double exchange (DE) interaction,[13-15] originating from Hund coupling between e_g and t_{2g} electrons, and the Jahn-Teller (JT) distortion, due to the orbital degeneracy of the e_g state, have been proposed for explaining the CMR effect.[16-18] The on-site Coulomb interaction between e_g electrons, however, must be important because these interactions are stronger in magnitude than Hund coupling and the JT splitting of the e_g states.[19] Actually, the on-site Coulomb interaction modifies the results obtained in the simple DE interaction,[20] and gives rise to a coupling between the spin and orbital degrees of freedom in combination with the orbital degeneracy.[7,21-23] This coupling has been pointed out to play an important role in the spin and orbital orderings of the undoped manganites in a mean field approximation.[24,25] In the following, we study the spin and orbital orderings and their excitations in the undoped insulating phase of $LaMnO_3$ and the charge-ordered phase with 50% doping, taking into account the on-site Coulomb interaction, Hund coupling, the degeneracy of e_g orbitals and the mixing between e_g orbitals.

Our starting model consists of the following terms: hopping integrals between $d_{x^2-y^2}$ and $d_{3z^2-r^2}$ orbitals on nearest-neighbor (n.n.) sites, Hund coupling between itinerant e_g and localized t_{2g} spins, on-site Coulomb interaction between e_g electrons, i.e., intra- and inter orbital Coulomb and inter orbital exchange interactions U, U' and J', respectively, and AF coupling between localized t_{2g} spins. Since U, U' and J' have the largest energy scales, we eliminate them in the usual second-order perturbation and obtain an effective Hamiltonian:[24,25]

$$H_{\rm eff} = \tilde{H}_t + \tilde{H}_{e_g} + H_K + H_{Jt_{2g}}. \quad (1)$$

The first term denotes the effective hopping of e_g electrons with a constraint prohibiting the double occupancy of the same site and is given as

$$\tilde{H}_t = \sum_{\langle ij\rangle\sigma\mu\nu} t_{ij}^{\mu\nu}\tilde{c}_{i\mu\sigma}^{\dagger}\tilde{c}_{j\nu\sigma} + \text{h.c.}, \quad (2)$$

where $\tilde{c}_{i\mu\sigma}(\tilde{c}_{i\mu\sigma}^{\dagger})$ is an annihilation (creation) operator of e_g electrons on site i, orbital μ with spin σ with the constraint. $t_{ij}^{\mu\nu}$ is a hopping integral between orbital μ on site i and orbital ν on site j. The second term in eq. (1) represents the effective interaction between e_g electrons, which includes the coupling between the spin and orbital degrees of freedom:

$$\begin{aligned}\tilde{H}_{e_g} = \frac{-2}{U'-J'}\sum_{\langle ij\rangle}\Big(\frac{3}{4}n_in_j + \boldsymbol{S}_i\cdot\boldsymbol{S}_j\Big)\times\Big[\Big(t_{ij}^{aa2}+t_{ij}^{bb2}\Big)\\ \Big(\frac{1}{4}n_in_j - T_i^zT_j^z\Big) + \Big(t_{ij}^{ab2}+t_{ij}^{ba2}\Big)\Big(\frac{1}{4}n_in_j + T_i^zT_j^z\Big)\\ -t_{ij}^{aa}t_{ij}^{bb}\Big(T_i^+T_j^- + T_i^-T_j^+\Big) - t_{ij}^{ab}t_{ij}^{ba}\Big(T_i^+T_j^+ + T_i^-T_j^-\Big)\\ -\Big(t_{ij}^{ba}t_{ij}^{aa} - t_{ij}^{ab}t_{ij}^{bb}\Big)\Big(T_i^+T_j^z + T_i^-T_j^z\Big)\\ -\Big(t_{ij}^{ab}t_{ij}^{aa} - t_{ij}^{ba}t_{ij}^{bb}\Big)\Big(T_i^zT_j^+ + T_i^zT_j^-\Big)\Big],\end{aligned} \quad (3)$$

where $\boldsymbol{S}$ and $\boldsymbol{T}$ are the spin and pseudospin operators representing the spin and orbital degrees of freedom of e_g electrons, respectively, and a and b stand for $d_{x^2-y^2}$ and $d_{3z^2-r^2}$ orbitals, respectively. The existence of terms such as $T_i^+T_j^-$, $T_i^+T_j^z$ and $T_i^+T_j^+$ can be understood when we note the exchange processes shown in Figs. 1(a), 1(b) and 1(c).

The role of $\tilde{H}_{e_g}$ will be explained later. The last two terms, H_K and $H_{t_{2g}}$, represent Hund coupling between the e_g and t_{2g} spins and AF coupling between the t_{2g} spins, and are given as $H_K = -K\sum_{i\mu\sigma_1\sigma_2}\boldsymbol{S}_i^{t_{2g}}\cdot\boldsymbol{S}_i$ and $H_{Jt_{2g}} = J_{t_{2g}}\sum_{\langle ij\rangle}\boldsymbol{S}_i^{t_{2g}}\cdot\boldsymbol{S}_j^{t_{2g}}$, respectively, where $\boldsymbol{S}_i^{t_{2g}}$ denotes the localized t_{2g} spin on the i site.

The effective Hamiltonian $\tilde{H}_{e_g}$ shows strong coupling between the spins and orbitals. The coupling is ferromagnetic in the spin space but antiferromagnetic in the orbital space, as seen in the z components of the orbital interaction in eq. (3). It is worth noting that the coupling constant is anisotropic because it depends on the hopping integrals t_{ij}^{ab}, which are anisotropic due to the character of the d-orbitals. The anisotropic F coupling between e_g spins competes to the isotropic AF coupling between t_{2g} spins, which will be the source of the variety of magnetic states discussed below.

In the undoped insulating phase, $\tilde{H}_t$ is neglected. Because Hund coupling is now the strongest interaction in the effective Hamiltonian and may make the e_g and t_{2g} spins parallel, we can introduce a supplementary isotropic AF interaction between e_g spins instead of H_K and $H_{Jt_{2g}}$ to represent the competing interactions between the antiferromagnetic $H_{Jt_{2g}}$ and the anisotropic ferromagnetic $\tilde{H}_{e_g}$. The resultant Hamiltonian for the insulating phase may be written as

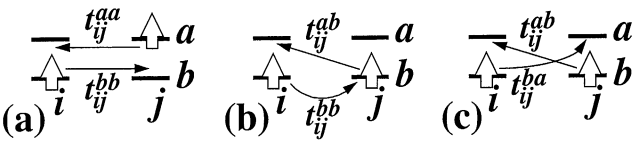

Fig. 1. Examples of the exchange processes to obtain the effective Hamiltonian $\tilde{H}_{e_g}$.

$$H_{\rm IS} = \tilde{H}_{e_g} + J_{\rm AF}\sum_{\langle ij\rangle}\boldsymbol{S}_i\cdot\boldsymbol{S}_j, \quad (4)$$

which is characterized by two parameters $\tilde{J} = t_0^2/(U'-J')$ and $J_{\rm AF}$. Here, t_0 is a hopping integral between n.n. $d_{x^2-y^2}$ orbitals in the x direction. The other integrals $t_{ij}^{\mu\nu}$ are expressed using t_0 in the tight-binding model. The Hamiltonian may be sufficient for describing the low-energy excitations. With this simplification, we can treat three-dimensional (3-D) 8-site ($2\times2\times2$) clusters using the ED method with the periodic boundary condition. One should note that the proper symmetry of the system is retained only when the 3-D is taken into account.

In Fig. 2, we show the phase diagram of the undoped insulator as a function of $J_{\rm AF}/\tilde{J}$ with calculated values of the spin correlation function $S(\boldsymbol{Q})$ with wave vector $\boldsymbol{Q}$. When $J_{\rm AF}/\tilde{J} < 1.0$, the total spin value $S^{\rm tot}$ has the maximum value $S_{\rm max}$, and the ground state (GS) is F. For $J_{\rm AF}/\tilde{J} > 1.0$, $S^{\rm tot} = 0$ and GS is AF. The types of AF ordering can be identified by the $\boldsymbol{Q}$ vector at which $S(\boldsymbol{Q})$ is maximum. As the $\boldsymbol{Q}$ vector changes from $\boldsymbol{Q} = (0,0,\pi),(0,\pi,\pi)$ to (π,π,π) with increasing $J_{\rm AF}/\tilde{J}$, the structure of the AF state changes in the order of A-, C- and G-type, as depicted in Fig. 2.

The type of orbital ordering can be identified by calculating the orbital correlations $\langle\boldsymbol{T}_i\cdot\boldsymbol{T}_j\rangle$. In F, C and G-type AF orderings, orbitals align antiferromagnetically, that is, the $d_{x^2-y^2}$ and $d_{3z^2-r^2}$ orbitals are occupied alternately, which is denoted as $(x^2-y^2, 3z^2-r^2)$ ordering, hereafter. In $(x^2-y^2, 3z^2-r^2)$ ordering, F coupling along the z-axis is stronger than that within the $x-y$ plane. Therefore, F ordering naturally changes to C- and G-type AF with increasing $J_{\rm AF}/\tilde{J}$. In this orbital ordering, however, the A-type AF does not appear. The A-type AF occurs only when the orbital ordering is rearranged to $(3y^2-r^2, 3x^2-r^2)$ ordering,[26] as shown in Fig. 3(a).

In this orbital ordering, F coupling along the z-axis is weaker than that in the $x-y$ plane. Therefore, the orbitals adjust themselves to lower the GS energy by creating four F bonds and two AF bonds in the A-type AF for small values of $J_{\rm AF}/\tilde{J}$. Actually, the orbital correlation of this ordering develops in the parameter region where the A-type AF is realized. In our previous work,[24,25] $(3y^2-r^2,\ 3x^2-r^2)$ orbital ordering was assumed to satisfy the observed lattice distortion.[27] Under this assumption, the occurence of the A-type AF has been explained in the mean field approximation. Using the ED method, however, the appearance of the A-type AF is self-consistently determined without the need for making any assumption. It should be stressed here that the A-type AF is realized due to the strong on-site Coulomb interaction and orbital degeneracy. Thus, we can see a strong interplay of spin and orbital orderings in the in-

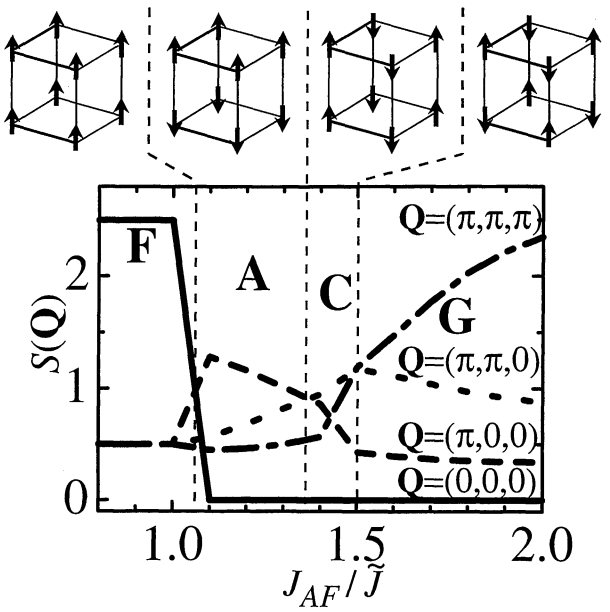

Fig. 2. The phase diagram of the insulating phase. Types of spin ordering and calculated values of the spin correlation functions $S(\boldsymbol{Q})$ with wave vector $\boldsymbol{Q}$ are shown as functions of $J_{\rm AF}/\tilde{J}$.

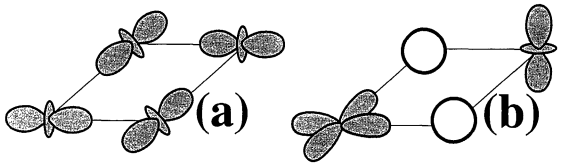

Fig. 3. Types of orbital orderings of the A-type AF (a) in the insulating phase and (b) in the charge-ordered phase with 50% doping.

sulating manganites.

The value of $J_{\rm AF}$ is estimated to be ~ 0.01 eV from the Néel temperature of $CaMnO_3$, taking into account the replacement of $H_{Jt_{2g}}$ with effective AF coupling between $S = 1/2$ e_g spins. Because the on-site Coulomb interaction is estimated to be $4 \sim 9$ eV from the photoemission experiments,[19] we obtain $J_{\rm AF}/\tilde{J} \sim 1$ if we assume that $|t_0| = 0.2 \sim 0.3$ eV. Therefore, the present results account for the A-type AF observed in $LaMnO_3$. The type of orbital ordering in the A-type AF is the same as that derived by the JT effect.[28,29] This suggests that the JT effect stabilizes the A-type AF cooperatively with the on-site Coulomb interaction in this case.

We have calculated the dynamical spin correlation functions $S(\boldsymbol{Q}, \omega)$ for F, A-, C- and G-type AF orderings in the ED method. We found that the spectra with strong intensity appear in the low-energy region, and incoherent spectra with weak intensity spread over the high-energy region. The incoherent spectra are caused by the coupled excitations of spins and orbitals. In spite of the coupling, the low-energy spectra are produced by the spin wave excitations.[24,25,30] The orbital excitations are rather difficult to analyze because the total angular momentum is not conserved, as can be seen in the Hamiltonian, therefore we omit detailed discussion of the orbital excitations.

Next, we study the charge-ordered state at 50% doping. Since the size of the unit cell for the ED study is limited, we focus our attention on how the interplay of spins and orbitals can be realized in NaCl-type charge ordering. This problem is highly nontrivial because the hopping of e_g electrons to a n.n. vacant site leads to a gain in the kinetic energy and produces additional interactions. The important point is that the kinetic energy depends on the orbital orderings. In this case, the e_g electrons are mobile and the simplification used for the undoped insulator cannot be allowed and thus the t_{2g} and e_g spins must be dealt with separately. We further add a term for n.n. Coulomb repulsion to realize NaCl-type charge ordering. Thus, the Hamiltonian is given by

$$H_{\rm CO} = H_{\rm eff} + V \sum_{\langle ij \rangle} n_i n_j, \tag{5}$$

where V denotes the n.n. Coulomb repulsion. Now the competing interactions are the AF interaction between t_{2g} spins, the F couplings due to the effective Hamiltionian derived for e_g electrons and the DE-type interaction caused by the hopping of e_g electrons. Here, we assume $1/2$ spin in place of t_{2g} spins to make the ED calculation possible for $2 \times 2 \times 2$ dice. We take relatively large values of $K = 10|t_0|$ and $V = 10|t_0|$ to ensure the parallel alignment of e_g and t_{2g} spins on the same site and the charge ordering, and take $\tilde{J} = 0.1|t_0|$.

The magnetic phase diagram is analized by calculating $S^{\rm tot}$ as a function of $J_{t_{2g}}/t_0$. F ordering occurs for $0 \leq J_{t_{2g}}/t_0 \lesssim 0.002$, which changes to AF ordering for $0.002 \lesssim x \lesssim 0.04$. Above $J_{t_{2g}}/t_0 \sim 0.04$, a ferrimagnetic (Ferri) ordering appears. In the Ferri state, spins of Mn^{3+} and Mn^{4+} align alternately, and $S^{\rm tot}$ becomes 2 for 8-site clusters. The GS is generally degenerate due to the e_g orbitals. However, the numerical calculation shows that the degeneracy is lifted at $J_{t_{2g}}/t_0 \sim 0.01$. The results of $S(\boldsymbol{Q})$ at this parameter value indicate that the spins are ordered in A-type AF. It is interesting to note that the degeneracy of the orbital part can be lifted by the spin part and A-type AF appears by the F states as in the undoped case.

In this A-type AF, the orbitals order within the $x-y$ plane as shown in Fig. 3(b). The ferromagnetic spin alignment and this orbital alignment within the $x-y$ plane are due to the virtual hopping of the e_g electrons, which leads to the DE-type F interaction, effective F coupling between e_g spins and AF orbital coupling in $\tilde{H}_{e_g}$. The result is also an indication of the interplay of spins and orbitals. The reason for the interlayer AF spin coupling, however, is rather difficult to analyze because the calculated orbital correlation functions do not give a classical picture of interplane orbital ordering. This may be due to the rather large quantum fluctuations in spin, orbital and charge degrees of freedom.

A realistic parameter value of $J_{t_{2g}}/|t_0|$ may be $0.03 \sim 0.05$, if $|t_0| = 0.2 \sim 0.3$ eV, because $J_{t_{2g}} \sim J_{\rm AF} \sim 0.01$ eV, as discussed for the insulating phase. Therefore, AF ordering may be realized as the observed spin structure.

It is interesting to note that the A-type AF structure has been observed for near 50% doped mangan-

ites. Moritomo[11] reports that A-type AF appears near the F phase in $(Nd\text{-}La)_{0.5}Sr_{0.5}MnO_3$, and Yoshizawa[12] shows that $Pr_{0.5}Sr_{0.5}MnO_3$ is an A-type AF. It has been pointed out that the average ionic radius $\langle r \rangle$ of R and A ions in $(R\text{-}A)MnO_3$ perovskites governs the magnetic properties,[3] and the F state is favorable when $\langle r \rangle$ is large. The experimental results mentioned above indicate that the F state may change to complex AF states via the A-type AF when the ionic radius is decreased on replacing Sr with Ca or La with Nd. Thus, the variety of magnetic orderings originating from the interplay of spins and orbitals calculated in this work may show a good correlation with the observed results.

In our results for $2 \times 2 \times 2$ clusters Ferri ordering has been obtained for strong AF coupling between t_{2g} spins, i.e., for weak effective coupling $\tilde{J}$. The latter corresponds to larger lattice distortion with smaller $\langle r \rangle$. Our results, therefore, indicate a possibility of observing Ferri ordering in regions with small ionic radius.

In conclusion, taking into account the strong on-site Coulomb interaction, orbital degeneracy and Hund coupling, we have studied the interplay of spins and orbitals for the undoped insulating and 50% doped charge-ordered phases using the ED method where the spin and orbital orderings were determined self-consistently. The interplay of spins and orbitals has been found to be crucial in such a way that the anisotropic magnetic structures are realized by self-adjustment of the orbital ordering when the orbital degeneracy is lifted by spins. The calculated results of the spin excitations in the insulating phase justify the analysis of neutron measurements in the spin wave approximation.[24,25,30] We stress the importance of the on-site Coulomb interaction and orbital degree of freedom in elucidating the magnetic properties as well as the CMR effect.

This work was supported by a Grant-in-Aid for Scientific Research on Priority Areas from the Ministry of Education, Science and Culture of Japan, and the New Energy and Industrial Technology Development Organization (NEDO). Computations were performed at the Computor Centers of the Institute of Molecular Science, Okazaki National Research Institute, Institute for Materials Research, Tohoku University and Institute for Solid State Physics, University of Tokyo.

1) R. von Helmolt, J. Wecker, B. Holzapfel, L. Schultz and K. Samwer: Phys. Rev. Lett. **71** (1993) 2331.
2) Y. Tokura, A. Urushibara, Y. Moritomo, T. Arima, A. Asamitsu, G. Kido and N. Furukawa: J. Phys. Soc. Jpn. **63** (1994) 3931.
3) H. Y. Hwang, S.-W. Cheong, P. G. Radaelli, M. Marezio and B. Batlogg: Phys. Rev. Lett. **75** (1995) 914.
4) Y. Tomioka, A. Asamitsu, Y. Moritomo, H. Kuwahara and Y. Tokura: Phys. Rev. Lett. **74** (1995) 5108.
5) Y. Tokura, Y. Tomioka, H. Kuwabara, A. Asamitsu, Y. Moritomo and M. Kasai: Physica C **263** (1996) 544.
6) E. O. Wollan and W. C. Koehler: Phys. Rev. **100** (1955) 545.
7) J. B. Goodenough: Phys. Rev. **100** (1955) 564.
8) P. Schiffer, A. P. Ramirez, W. Bao and S.-W. Cheong: Phys. Rev. Lett. **75** (1995) 3336.
9) Z. Jirák, S. Krupička, Z. Šimša, M. Ddouhá, and S. Vratislov: J. Magn. Magn. Mater. **53** (1985) 153.
10) H. Kuwahara, Y. Tomioka, Y. Moritomo, A. Asamitsu, M. Kasai, R. Kumai, Y. Tokura: Science **272** (1996) 80.
11) Y. Moritomo: Phys. Rev. B in press.
12) H. Yoshizawa: to be published.
13) C. Zener: Phys. Rev. **82** (1951) 403.
14) P. W. Anderson and H. Hasegawa: Phys. Rev. **100** (1955) 675.
15) P.-G. de Gennes: Phys. Rev. **118** (1960) 141.
16) N. Furukawa: J. Phys. Soc. Jpn. **63** (1994) 3214.
17) A. J. Millis, P. B. Littlewood and B. I. Shraiman: Phys. Rev. Lett. **74** (1995) 5144.
18) H. Röder, J. Zang and A. R. Bishop: Phys. Rev. Lett. **76** (1996) 1356.
19) S. Saitoh, A. E. Bocquet, T. Mizokawa, H. Namatame, A. Fujimori, M. Abbate, Y. Takeda and M. Takano: Phys. Rev. B **51** (1995) 13942.
20) J. Inoue and S. Maekawa: Phys. Rev. Lett. **74** (1995) 3407.
21) J. Kanamori: J. Phys. Chem. Solids. **10** (1959) 87.
22) K. I. Kugel' and D. I. Khomskiĭ: JETP Lett. **15** (1972) 446.
23) T. M. Rice: *Springer Series in Solid-State Sciences*, ed. A. Fujimori and Y. Tokura (1995) Vol. 119, p. 221.
24) S. Ishihara, J. Inoue and S. Maekawa: Physica C **263** (1996) 130, and references therein.
25) S. Ishihara, J. Inoue and S. Maekawa: Phys. Rev. B **55** (1997) No. 13.
26) Within the present Hamiltonian, $(z^2 - x^2,\ y^2 - z^2)$ ordering is equivalent to $(3y^2 - r^2,\ 3z^2 - r^2)$ ordering.
27) G. Matsumoto: J. Phys. Soc. Jpn. **29** (1970) 606.
28) T. Mizokawa and A. Fujimori: Phys. Rev. B **51** (1995) 12880.
29) I. Solovyev, N. Hamada and K. Terakura: Phys. Rev. Lett. **76** (1996) 4825.
30) K. Hirota, N. Kaneko, A. Nishizawa and Y. Endoh: J. Phys. Soc. Jpn. **65** (1996) 3736.